UNIVERSIDAD DE CÓRDOBA

Facultad de Ciencias

Titulación

Trabajo Fin de Grado

Título del Trabajo Fin de Grado

Código del TFG: **Código asignado a este TFG**

Tipo de TFG: **Tipología del trabajo**

Autor: Nombre y apellidos del autor

Fecha de entrega

Agradecimientos

Incluir los agradecimientos, si procede.

Contents

Índice de figuras

List of Tables

Resumen

Escriba aquí un resumen de la memoria en castellano que contenga entre 100 y 300 palabras. Las palabras clave serán entre 3 y 6.

Palabras clave: palabra clave 1; palabra clave 2; palabra clave 3; palabra clave 4

Abstract

Insert here the abstract of the report with an extension between 100 and 300 words.

Keywords: keyword1; keyword2; keyword3; keyword4

CHAPTER 1

Introduction

1.1. The Hot Big Bang model

The most accepted model for the origin of the universe is the Big Bang model, that models the beginning of the universe as a hot dense state. The Big Bang surprisingly to some conveys no "bang", but the sudden existence of all the matter in the universe, in the shortest of times, in the smallest of spaces, about 13.8 billion years ago. After an unthinkably small interval of time, the universe began a short period of rapid expansion known as *cosmic inflation*, in which the universe grew by a factor 10^{27} in a mere 10^{-33} seconds. This inflation is thought to be due to the inflaton, a quantum scalar field. It is theorized that it is the inflaton's vaccuum energy what caused the universe to expand as greatly.

As any quantum field[1] the inflaton presents fluctuations. This means, even in the vacuum state[2] there is constant creation and annihilation of particles. These fluctuations are what cause anisotropies in the matter distribution of the universe, fact that will be important later in this work.

After the inflation phase, the universe cooled enough for what is known as the Quark-Gluon plasma to form. In this state, temperatures were high enough as to consider relativistic the random motion of the particles in it. After some cooling due to cosmic expansion, the combination between quarks to form hadrons was allowed, leading to what is known as the hadronic epoch. However, due to the short mean free path of the photons, the universe is still opaque to electromagnetic radiation.

As the universe kept expanding the densities decreased and the temperatures cooled,

[1] Quantum fields are a tool used by Quantum Field Theory (QFT) to more accurately describe particles and their interactions, at high enough energies.

[2] To define vacuum in QFT is not as easy a task as it was in classical mechanics (or even non-relativistic quantum mechanics).These details go beyond the scope of this paper, and thus will not be dealt with.

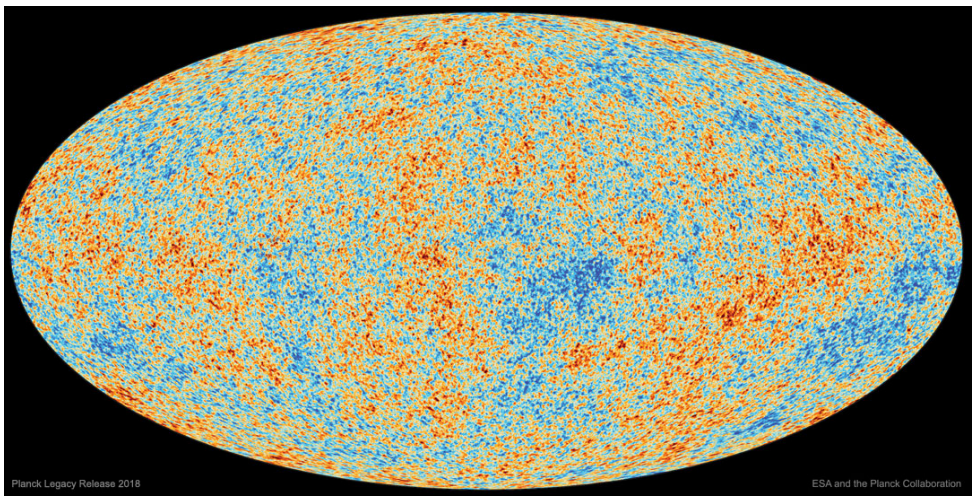

Figura 1.1: The all-sky map of CMB anisotropies as seen by Space-based Observatory Planck [1]. The colors in this map represent the fluctuations of the mean T = 2.7 K with fluctuations of 10^{-5} with respect to the average temperature. Red means higher temperature than the average, whilst blue means lower temperature than the average.

the existence of atoms was starting to be allowed, the He and H atoms. This period would finish at the universe age of 380,000 years, moment known as recombination. Recombination is thought of as the time at which the Thomson Scattering mechanisms stop being effective (the scattering cross section of this process becomes negligible and thus the photon mean free path grows considerably). As soon as recombination ends, the thermally activated photons which are no longer energetic enough to interact with the electrons now travel freely through space. This emission is known as the Cosmic Microwave Background (CMB) and is the oldest direct observation using electromagnetic radiation we can take of the universe.

Though the name 'recombination' implies the fact that the universe used to be 'combined' and then ceased to be so, it just comes from the fact that recombination was theorized before the Big Bang theory was thought of.

1.2. Cosmic Microwave Background

We see in the figure 1.1 the CMB as observed by the Planck colaboration [1]. The radiaton we observe is the photons that were emmitted about 13.8 billion years ago. Since the CMB appears as a result of the thermal photons emitted by the electrons in the primordial plasma, it offers great insight into what the plasma looked like, and the way it behaved.

The Cosmic Microwave Background was discovered in 1965 as a serendipity by Penzias and Wilson [2]. They observed a noise signal, uniformly distributed[3] from every direction, day or night, summer or winter, almost as if it came directly from the origin of the

[3]It was not actually uniformly distributed, since there was a small doppler shift due to the Earth's

universe. This discovery was considered to be solid evidence for the Big Bang model and more importantly, the beginning of the modern cosmology. All of this became the reason Penzias and Wilson received a Nobel prize 13 years later, in 1978.

Since what is being measured are the photons left from recombination, which corresponds to a thermal radiation curve, we may use Wien's displacement law

$$T = \frac{b}{\lambda} \tag{1.1}$$

with $b \approx 2.897\,\text{mmK}$ Wien's constant, T the black body radiation and λ the wavelength at which the spectral radiation intensity is maximum to calculate the corresponding temperature to the measured wavelength. Using Planck's law, the measured temperature is 2.7 K which corresponds to a measured wavelength of 1.06 mm (microwave radiation, as the name Cosmic *Microwave* implies).

In 1991 anisotropies in the CMB were first discovered, by the COBE satellite[3] later earning Smoot and Mather a nobel prize. As of 2023 the most precise measurements correspond to the Planck experiment in 2018 [1] by the European Space Agency. These anisotropies can be seen in 1.1.

Of course, 2.7 K was not the temperature of the plasma at recombination, as it was approximately hotter by a factor $z = 1090$, or $\approx$3000 K. The reason we measure such smaller temperatures is because of the expansion of the universe.
If today ($t = t_0$) some radiation of wavelength λ_o is observed, that somehow is known to have been travelling for some time Δt will have stretched due to the expansion of the universe. In other words, the wavelength λ_e of the emitted radiation was smaller by a factor[4] $a(t')^{-1}$, with $t' = t_0 - \Delta t$ being the earlier time at which the radiation was emitted, and $a(t_0) = 1$ by definition. By Wien's displacement law (1.1), this corresponds to a higher temperature by a factor $a(t')$.

Thus, the CMB becomes crucial in explaining the large scale structure of the universe, since the photons that decoupled from the plasma at recombination wasted more energy leaving denser regions behind losing thermal energy in the process. Appearing at a slightly lower temperature (gravitational redshift). On the contrary, those in void regions will appear hotter, being blueshifted. Therefore, temperature fluctiations in the CMB correspond to density fluctuations in the early universe.

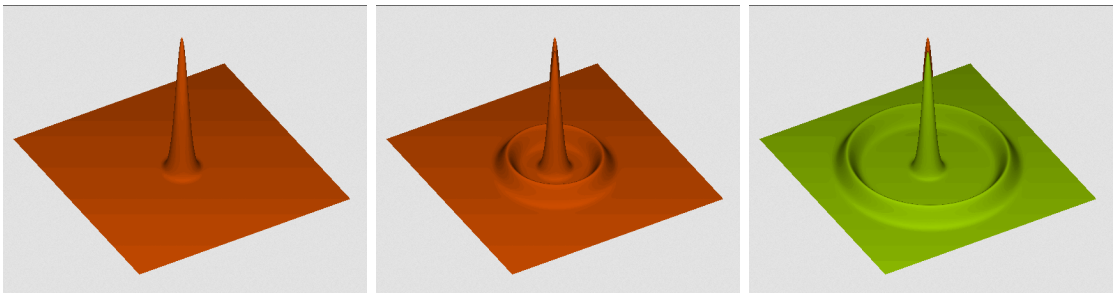

(a) Origin of the BAO (b) The BAO propagating through the plasma (c) The frozen BAO after recombination

Figura 1.2: Different stages of the Baryon Acoustic Oscillations. Courtesy of the image (cite https://lweb.cfa.harvard.edu/ deisenst/acousticpeak/anim.gif)

1.3. Baryon Acoustic Oscillations

Before recombination, both matter and photons were coupled into the same fluid which we have called the primordial plasma. The particles in the plasma interacted primarily with one another through gravity and electromagnetism, depending on the type of matter considered.

As already mentioned, matter was not distributed homogenously. At some point in time before recombination one could find 'lumps' of dark and baryonic (standard) matter. Combining the restoring force of the gravitational attraction between dark and baryonic matter with itself and with one another, and the repulsion caused by the radiation pressure due to the Thomson Effect between baryons and photons, the results are pure acoustic waves propagating through the plasma, with the dark matter lumps being in the center of these waves. Since the baryonic matter is dragged by these sound waves, they are called Baryon Acoustic Oscillations (BAO).

The waves would propagate throughout the plasma as long as the baryon-photon interaction was strong enough i.e. up to recombination, at which point they froze in time leaving higher density regions. Higher density means higher gravitational intensity, which in turn means higher galaxy proliferation in spherical distributions. These spherical distributions (which can be measured in the CMB) are what is known as the large scale structure of the universe.

At big enough distances, the radii (r_s) of these spheres, also called the sound horizon is used as a 'cosmic ruler'. Big scale measurements are calculated in terms of r_s, which is measured from the CMB. This means it needs to be calibrated from external information.

relative movement to the CMB. Surprisingly, even after removing this and other similar effects, it still presents minute fluctuations. These fluctuations, as it will be seen in the next sections contain a great deal of information on the composition of the universe and explains the origin of structure formation.

[4]The factor $a(t)$ is known as the scale factor of the universe, and will be explained with further detail later in the work.

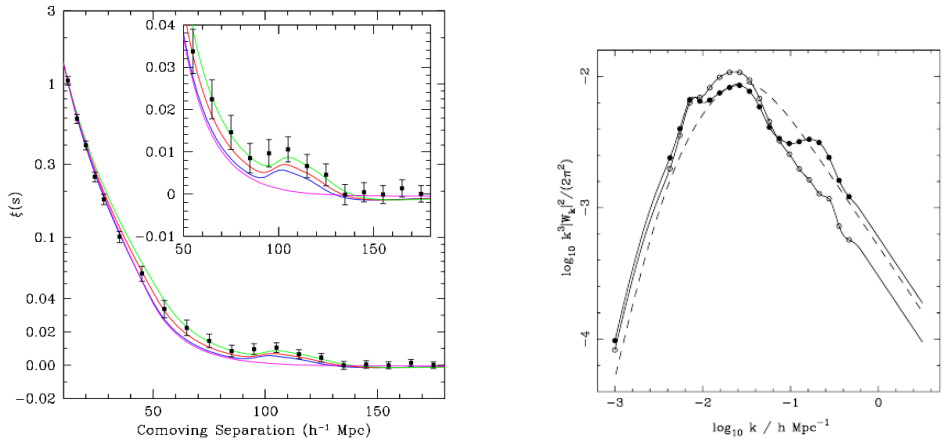

(a) The correlation function $\xi(s)$ as measured by the Sloan Digital Sky Survey [5]

(b) The power spectrum as observed by the 2dF collaboration [4]

Figura 1.3: First detections of BAO

r_s has been measured from the CMB to be around 150 Mpc or 500 million lightyears. To give an idea of the size of r_s, the radius of the observable universe is around 100 times r_s.

Given the large dimensions of this cosmic ruler and the homogeneity of the universe on large scales, this ruler is only affected by cosmological expansion rather than late-time gravitational effects. Therefore, it has a constant comoving[5] size throughout the universe.

These structures were observed for the first time in 2005 simultaneously both by the 2dF Galaxy Redshift Survey[4] and the Sloan Digital Sky Survey[5], the results of which can be seen in the figure 1.3. In these pictures one sees the correlation function $\xi(r)$ and the power spectrum $P(k)$ (though in the figure 1.3(b) it is called W_k). These are the main tools for the study of the BAO. The correlation function $\xi(s)$, with s being a distance variable measures the frequency of the separation between any two galaxies. If the BAO hypothesis is true, then one would find a local maximum at r_s, the radius of the frozen spherical waves.

The other tool for studying the BAO is the power spectrum seen in 1.3(b). It is, without need of more detail, the Fourier transform of the $\xi(s)$ function. Indeed, since there is a repeating pattern of wavelength r_s, one would find local maxima in the spectrum at integer multiples of $k = 2\pi/r_s$.

1.4. Curvature, dark matter and the expansion of the universe

After Hubble discovered the expansion of the universe through Hubble's Law[6]

$$v = H_0 d \tag{1.2}$$

[5] 'Comoving' meaning the distance one would measure had the expansion of the universe not existed

With v the recession speed (the speed at which some point in space is receeding only considering the expansion of the universe), $H_0 = 100h$ km s^{-1} Mpc^{-1} Hubble's constant, h a factor that parametrizes our ignorance on the true value of H_0 (estimated to be around 0.67), and d the distance of said point, a great deal of studies concerning the expansion of the universe started. The most relevant result of those for this report are Friedmann's equations.

$$H^2(t) := \left(\frac{\dot{a}}{a}\right)^2 = \frac{8\pi G\rho}{3} + \frac{\Lambda c^2}{3} - k\frac{c^2}{a^2} \tag{1.3}$$

$$3\frac{\ddot{a}}{a} = \Lambda c^2 - 4\pi G\left(\rho + \frac{3p}{c^2}\right) \tag{1.4}$$

In these equations we see many new parameters. $H(t)$ is a generalization of H_0, H_0 being the value of $H(t)$ at $t = t_0$ where t_0 is the age of the universe. $a(t)$ is the scale factor of the universe, meaning that if a certain length measurement Δx was taken at time t_1, then that same measurement would be $\frac{a(t_2)}{a(t_1)}\Delta x$ at t_2. G is the Newton's gravitational constant, ρ the density of the universe (including baryonic, dark matter, radiation and neutrinos), Λ is the cosmological constant which contains information about Dark Energy. Finally we see k, which is the spatial (Gaussian) curvature of the universe. This is, asymptotical curvature.

These equations are a result of the Friedmann–Lemaître–Robertson–Walker metric

$$ds^2 = -c^2dt^2 + a^2(t)\left(\frac{dr^2}{1-kr^2} + r^2d\theta^2 + r^2\sin^2\theta d\phi^2\right) \tag{1.5}$$

which are a direct result of solutions to Einstein's field equations of General Relativity, which will not be covered in this work. In (1.5) one sees the usual components in a flat space Minkowskian metric

$$ds^2 = -c^2dt^2 + dr^2 + r^2d\theta^2 + r^2\sin^2\theta d\phi^2 \tag{1.6}$$

and some new terms, $a(t)$ and k. $a(t)$ is the aforementioned scale factor, and k a measure of the curvature of the universe. It is easier now to see that $a(t)$ is crucial in the way lengths are measured, being an overall factor in the spatial part that is homogeneues but time-dependent. Also, one can notice how having different types of universe affects differently to the metric. For example $k = 0$ yields (as one would expect) a flat universe. $k > 0$ corresponds to a universe with spherical geometry and $k < 0$ to a universe of hyperbolical geometry.

If one managed to solve (1.3), the result would be $a(t)$, a description of the history of the expansion of the universe. Moreover, it is also important to notice the relationship between the expansion of the universe and the distribution of matter in the universe.

From (1.3) we define the density parameter Ω_m as $\frac{\rho}{\rho_c}$, with the critical density $\rho_c = \frac{3H_0^2}{8\pi G}$, which represents the transition point (for a universe without cosmological constant) between an ever expanding universe with negative curvature (open universe) and a collapsing universe with positive curvature (closed universe). Similarly from the rest of the terms in the equation (1.3)

$$\Omega_\Lambda = \frac{\Lambda c^2}{3H^2}, \Omega_k = -\frac{kc^2}{H^2a^2} \tag{1.7}$$

Ω_Λ corresponds to the density of dark energy in the universe, while Ω_k is not a density *per se*, but is related to the total energy content of the universe, determining its curvature. These parameters are what define the certain cosmology we are using, and obey the cosmic sum rule

$$1 = \Omega_m + \Omega_\Lambda + \Omega_k \tag{1.8}$$

Which is just a result of dividing (1.3) evaluated at present time, by H_0^2.

Historically, the concept of cosmological expansion appeared when Hubble observed that the radiation of the nearby galaxies was all shifted towards the red end of the spectrum. Of course, since the universe is expanding and the distance between two points increases with time, the wave length of a certain radiation would also be affected by this expansion. This stretching of the wave length is what is known as *redshift*

$$z = \frac{\lambda_\mathrm{o} - \lambda_\mathrm{e}}{\lambda_\mathrm{e}} = \frac{\lambda_o}{\lambda_e} - 1 \tag{1.9}$$

Being λ_o the observed wavelength and λ_e the emitted wavelength of the considered radiation. z is a measure of how much the universe stretched while the radiation travelled, and it can be related to $a(t)$ through

$$\frac{\lambda_o}{\lambda_e} = 1 + z = \frac{a(t_o)}{a(t_e)} \tag{1.10}$$

Which means that z is a temporal variable measuring the time the radiation travelled through the universe.

However, this redshift z should not be confused with the redshift caused by the Doppler Effect of objects moving away. The processes are different in origin, since cosmological redshift does not need relative movement to shift the radiation towards red wavelengths, it is the expansion of the universe what stretches the wavelength. On the contrary, the Doppler Effect appears when pulses emmitted at regular time are emitted further away due to the movement of the wave source.

We thus define the comoving distance $\Delta x'$ of a measurement Δx as

$$\Delta x' = \frac{\Delta x}{a(t)} = (1+z)\Delta x \tag{1.11}$$

i.e. the distance one would have measured had the expansion of the universe not existed.

With these definitions we can define the observables we are interested in calculating/measuring. Firstly, through (1.3) we calculate $H(z)$ as

$$H(z) = H_0\sqrt{\Omega_m(1+z)^3 + \Omega_k(1+z)^2 + \Omega_\Lambda} \tag{1.12}$$

We also define the function of z $D_H(z)$ known as the Hubble distance

$$D_H(z) = \frac{c}{H(z)} \tag{1.13}$$

Note that for $z = 0$ D_H gives us an idea of the distance at which the recession speed is greater than the speed of light in the vacuum, which is a direct consequence of (1.2). D_H

can also be used to estimate the order of magnitud of the observable universe.

Through the Hubble distance we define the comoving distance

$$D_C(z) = \frac{c}{H_0} \int_0^z \frac{dz'}{\sqrt{\Omega_m(1+z')^3 + \Omega_k(1+z')^2 + \Omega_\Lambda}} \tag{1.14}$$

From this expression one defines the angular diameter distance for some redshift z

$$D_A(z) = \begin{cases} \frac{D_H}{(1+z)\sqrt{\Omega_k}} \sinh\left[\sqrt{\Omega_k} D_C/D_H\right] & \Omega_k > 0 \\ \frac{1}{1+z} D_C & \Omega_k = 0 \\ \frac{D_H}{(1+z)\sqrt{|\Omega_k|}} \sin\left[\sqrt{|\Omega_k|} D_C/D_H\right] & \Omega_k < 0 \end{cases} \tag{1.15}$$

1.5. Λ Cold Dark Matter model

In the definitions in (1.7) the parameters Ω were introduced. This definitions, plus the definition of the density parameter Ω_m are part of the set of parameters that form the Λ Cold Dark Matter (ΛCDM) model.

This model is the simplest available way of explaining the current state of the universe, with 6 different constants. The name is derived from two of the biggest components of the universe, Λ (the cosmological constant, related to Dark Energy) and Cold Dark Matter, which is thought to be

- **Cold**: Non relativistic ($v \ll c$)
- **Non baryonic**: Made up of non baryonic matter i.e. anything other than protons and neutrons (and by convention, electrons).
- **Disipationless**: Since Dark Matter does not interact with the electromagnetic field, it can not dissipate temperature through photon emission.
- **Collisionless**: Dark matter particles can only interact through gravity and possibly, the weak force and so they do not collide with one another.

The information on this cold dark matter is inside Ω_m, since the density ρ in

$$\Omega_m = \frac{\rho}{\rho_c} = \frac{\rho_b + \rho_{\text{CDM}}}{\rho_c} \tag{1.16}$$

Allowing us to define two new density parameters $\Omega_b = \frac{\rho_b}{\rho_c}$ and $\Omega_c = \frac{\rho_{\text{CDM}}}{\rho}$, which are part of the six free parameters that define a certain cosmology. These are Ω_b, Ω_c, H_0, the optical density of reionization τ_{reio}, the amplitude of the primordial power spectrum A_s, the spectral index of the primordial power spectrum n_s. Note there is no special choice of parameters, these are just the free parameters chosen for this work.

In this work, an extension of the ΛCDM model is considered. Though the standard cosmological model considers a flat universe, the curvature parameter will not be fixed to 0 and is therefore allowed to be a free parameter, adding a new degree of freedom to the standard model (not to be confused with the particle physics standard model). This

model can be further extended by considering the mass of the neutrinos, the quintaessential force (dark energy)...

The fiducial (starting) values of these parameters that will be used in this work are

- $\Omega_b = 0.0481$
- $\Omega_c = 0.2604$
- $H_0 = 67.6$ km s^{-1} Mpc^{-1}
- $\tau_{\text{reio}} = 0.09$
- $A_s = 2.04031526769 \cdot 10^{-9}$
- $n_s = 0.97$

And Ω_k that will vary between -0.2 and 0.2.

From these free parameters, one derives some parameters. Of those, the main interest is in Ω_Λ, r_s, D_H, and D_A,

- $r_s = 147.784$ Mpc
- $D_H/r_s = 18.7$
- $D_A/r_s = 18.3$

And Ω_Λ will vary between 0.49 and 0.89.

Finally, we define two more parameters $\alpha_\parallel$ and $\alpha_\perp$. These parameters measure the distortion of the measurements in two different directions. $\alpha_\parallel$ is related to the distortion parallel to the line of sight, and $\alpha_\perp$, perpendicular to the line of sight. They are defined by

$$\alpha_\parallel = \frac{[D_H(z)/r_s]}{[D_H(z)/r_s]^{\text{fid}}},\ \alpha_\perp = \frac{[D_A(z)/r_s]}{[D_A(z)/r_s]^{\text{fid}}} \tag{1.17}$$

z being the redshift at which the measurements were taken.

CHAPTER 2

Objectives

The general objective of this final degree work is to study the behavior of baryon acoustic oscillation (BAO) observables, namely the sound horizon distance r_s, the Hubble parameter distance D_H, and the angular diameter distance D_A, as a function of the curvature parameter Ω_k. To achieve this objective, the following specific objectives are proposed:

1. Review the theoretical background of BAO observables, including their physical origin and mathematical formulation, and become familiar with the software tools Rustico, BRASS, and Python for data analysis and visualization.
2. Learn to use these software tools for data preprocessing, analysis, and visualization of BAO-related cosmological data sets, particularly those related to the curvature parameter Ω_k.
3. Investigate the impact of different values of Ω_k on the behavior of BAO observables.
4. Analyze the most recent observational data on BAO observables, obtained from experiments such as SDSS, BOSS, and eBOSS, and compare the results with theoretical predictions for different values of Ω_k.
5. Make use of high performance computing to solve Physics problems.
6. Specific data analysis software development.
7. Learn to control computer clusters via ssh.

Together, these objectives will provide a comprehensive understanding of the behavior of BAO observables for different values of Ω_k, and their role in constraining the curvature parameter and other cosmological parameters.

CHAPTER 3

Methods and materials.

For this work, many diferent tools were used, which will be cathegorized in hardware, software and mathematical tools.

In terms of hardware, the author was granted access to the *FQM-378* clusters in the Universidad de Córdoba. Access to these clusters was crucial for the calculations done throughout the work, reducing the time needed for each calculation in several orders of magnitude. Besides the clusters, the author also needed his own personal computer, mainly to remotely access the clusters and also for other types of calculations that could not have been done from the clusters. These calculations include among other things, plotting of figures.

The main mathematical tool for this work was the Fourier Transform. The Fourier Transform is a consequence of Fourier's Theorem. This theorem states that for every 'nice'[1] periodic function $f(x)$ of period L one can find a unique linear combination of sine and cosine functions such that

$$f(x) = C + \sum_{\text{n odd}} a_n \sin\left(\frac{nx}{L}\right) + \sum_{\text{n even}} b_n \cos\left(\frac{nx}{L}\right) \tag{3.1}$$

With C, a_n, b_n given by[2]

$$\begin{cases} C & = \frac{1}{L}\int_L f(x)dx \\ a_n & = \frac{1}{L}\int_L f(x)\sin\left(2\pi\frac{nx}{L}\right)dx, \text{ n odd} \\ b_n & = \frac{1}{L}\int_L f(x)\cos\left(2\pi\frac{nx}{L}\right)dx, \text{ n even} \end{cases} \tag{3.2}$$

[1] The conditions for which this theorem does not apply are beyond the scope of this work, and so the 'niceness' of a function need not be defined

[2] The subscript in $\int_L$ only implies the integration over the length L, since it can be proven that any periodic function $f(x)$ with period L verifies $\int_0^L f(x)dx = \int_a^{L+a} f(x)dx$ for any value of a. This is, the point at which the integral begins makes no difference, as long as the integration is done over a whole period.

This was the original Fourier's result. However this theorem can be expanded to the complex realm as

$$f(x) = \sum_{n=0}^{\infty} c_n e^{i2\pi \frac{nx}{L}}, \text{with } c_n = \frac{1}{L}\int_L f(x) e^{-i2\pi \frac{nx}{L}} dx \tag{3.3}$$

For each mode n one can define a new variable $k = 2\pi n/L$, leading to the actual definition of the Fourier Transform

$$\tilde{f}(k) = \frac{1}{2\pi}\int_L f(x) e^{-ikx} dx \tag{3.4}$$

In this work, the power spectrum $P(k)$ is considered, which is the Fourier Transform of the correlation function $\xi(r)$. Recalling the definition of the $\xi(r)$ function, the frequency of the distance at which two any two galaxies are found, one can notice that $\xi(r)$ must be a discrete function. We thus define the Discrete Fourier Transform (DFT) over a discrete set of N data points $\{(x_i, \xi(x_i))\}_{i=1}^{N}$

$$P(k_j) = \frac{1}{2\pi}\sum_{i=1}^{N} e^{-ik_j x_i}\xi(x_i) \tag{3.5}$$

Though one must think that the periodic function hypothesis is being broken, since of course the universe is not made of repeating blocks of the galaxies that surround us. That the universe is infinitely big and repeating is an assumption that needs to be done in order to calculate this Fourier Transform. In other words, these calculations asume periodic boundary conditions.

Another thing to be noted is the fast growing complexity of the algorithm described by (3.5), which grows as N^2, with N the number of points used for the calculation. To solve this one would use the Fast Fourier Transform (FFT), instead of the DFT. This algorithm is based in the decomposition of the space considered with $N = N_1 N_2$ data points, into two smaller spaces with N_1 and N_2 data points. It then factorizes each problem into smaller problems, and recursively breaks the configuration down into even smaller problems, thus greatly reducing the complexity of the algorithm from N^2 to $N \log N$.

The $P(k)$ has been until now only been vaguely defined. Let $\rho(\mathbf{x})$ determine the density of galaxies at a given point and $\overline{\rho}$ the average density throughout the universe. As the interest lays in the fluctuations around the density, it is only natural to be interested in the overdensity $\delta(\mathbf{x})$ at some position $\mathbf{x}$

$$\delta(\mathbf{x}) = \frac{\rho(\mathbf{x}) - \overline{\rho}}{\overline{\rho}} \tag{3.6}$$

From this magnitude one calculates the aforementioned correlation function $\xi(\mathbf{r})$ as[3]

$$\xi(\mathbf{r}) = \langle \delta(\mathbf{x})\delta(\mathbf{x}')\rangle = \frac{1}{V}\int_V d^3\mathbf{x}\delta(\mathbf{x})\delta(\mathbf{x}-\mathbf{r}) \tag{3.7}$$

with $\mathbf{r} = \mathbf{x} - \mathbf{x}'$ And the power spectrum is then defined as its three dimensional Fourier Transform.

[3]Note only the dependency on $r = \|\mathbf{r}\|$ remains, since the universe is (assumed to be) homogenous and isotropic

To calculate $P(k)$ one then needs three coordinates for each galaxy (as would be expected from a three dimensional universe). These coordinates will be 2 angular coordinates (the declination δ and right ascension α) and a radial coordinate r which must be calculated from z. For this it is necessary to assume a cosmology, since it is what dictates the conversion from redshift to distance through Hubble's law (1.2). For this transformation, the redshift is interpreted as a Doppler shift. At low enough velocities, $z \approx v/c$ and so (1.2) can be approximated to

$$cz = H_0 r \tag{3.8}$$

The last step to calculate the power spectrum is to interpolate in between each galaxy, similar to how one would build a heatmap. This way the catalogue is continuous and no longer discrete. Now, with a continuous density function $\rho(\mathbf{x})$ all necessities for the power spectrum are met and it can be finally calculated.

All these magnitudes are related to what is called the second moment of the overdensity. In general, the nth moment μ_n of some magnitude x with a probability distribution $P(x)$ is defined as

$$\mu_n = \int_{-\infty}^{\infty} x^n P(x) dx \tag{3.9}$$

It is then natural to ask why is only the second moment of the overdensity δ considered.[4] It has been measured in the CMB that the universe is a gaussian field. These kinds of fields have the property that any moment μ_n with $n > 2$ will be 0. These moments (e.g. $\langle \delta(\mathbf{x})\delta(\mathbf{y})\delta(\mathbf{z}) \rangle$) have been shown to all be compatible with 0. This is predicted by the inflation theory, but the strongest reason to believe this is the experimental data.

All these calculations are performed by Rapid foUrier STatIstics COde (RUSTICO)[9]. This software needs the specific galaxy catalogue to be used, and the statement of the cosmology that is going to be used, in a similar fashion as was done in 1.5. The catalogue to be used in this work is the Luminous Red Galaxy sample from the extended Baryon Oscillation Spectroscopic Survey (LRG eBOSS [11]). With this information it then takes the mentioned steps: Transforms each redshift z to a radial distance r, assigns each galaxy to a point $\mathbf{x}$, calculates through interpolation the galaxy density at each point $\rho(\mathbf{x})$, the overdensity at each point $\delta(\mathbf{x})$, the correlation function $\xi(r)$ and finally its FFT to obtain the power spectrum $P(k)$, as seen in the figure 3.1.

Having the data, it is then necessary to have a model that explains it. The Cosmic Linear Anisotropy Solving System (CLASS) [7] library allows the user to calculate the theoretical curve $P(k)$ should have for each cosmology. This software takes the corresponding cosmology as an input and returns the power spectrum seen in the leftmost panel of the figure 3.2. Note that this curve looks like a decreasing function which will be named $P_{\text{smooth}}(k)$, modulated by an oscilating curve, named $O_{\text{lin}}(k)$. These two functions are seen in the two leftmost panels of the figure 3.2, and verify

$$P(k) = P_{\text{smooth}}(k) O_{\text{lin}}(k) \tag{3.10}$$

[4] The dependency on $\mathbf{x}$ was dropped since δ can be both spoken of in configuration space and momentum (Fourier) space. These representations correspond to the $\xi(r)$ and $P(k)$ functions, respectively.

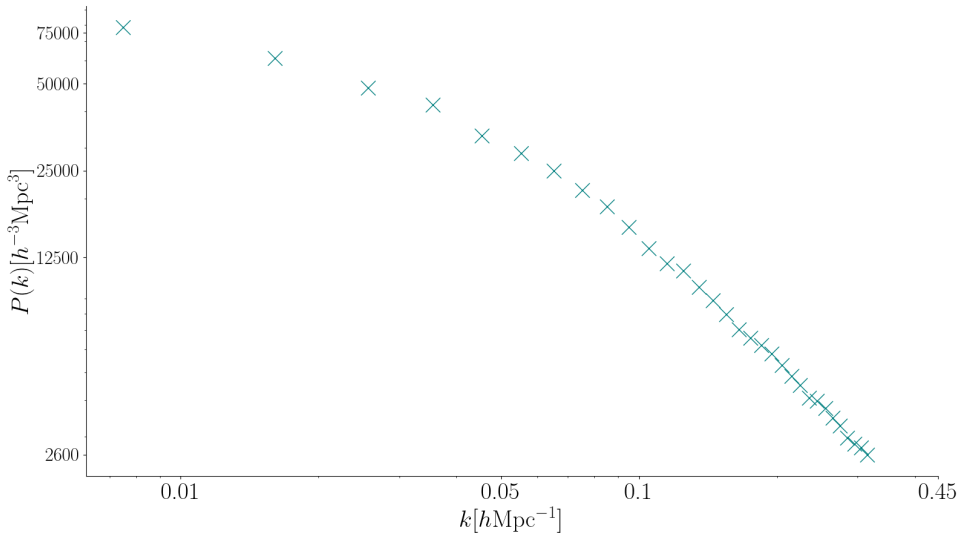

Figura 3.1: The power spectrum $P(k)$ of the LRG eBOSS [11] catalogue as calculated by RUSTICO ($\Omega_k = 0.00$)

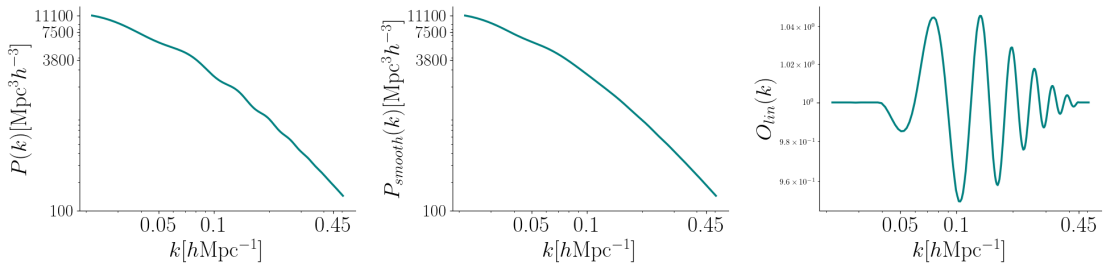

Figura 3.2: Graphic representation of the $P(k)$ (left panel), $P_{smooth}(k)$ (middle panel) and $O_{lin}(k)$ (right panel)for $\Omega_k = 0$.

To split the power spectrum $P(k)$ into these two functions, the routine *remove_bao* from the Montepython project [8] has been used. This routine takes as input the power spectrum $P(k)$ as an array of points. It then computes the geometrical curvature of the curve and interpolates in between the points at which the calculated curvature results in 0. The output of this function is the smoothed power spectrum $P_{\mathrm{smooth}}(k)$. By the definition (3.10), the pure BAO $O_{\mathrm{lin}}(k)$ are calculated through

$$O_{\mathrm{lin}}(k) = \frac{P(k)}{P_{\mathrm{smooth}(k)}} \tag{3.11}$$

The relationship between the data and the model is done through the Bao and RSD Algorithm for Spectroscopy Surveys (BRASS) [10]. This software allows for the calculation of the α parameters, as defined by (1.17). BRASS takes as input the calculated power spectrum (given by RUSTICO) for some fiducial cosmology, and the theoretic power spectrum for some other fiducial cosmology. It will return among many other fit parameters, the $\alpha_{\parallel}$ and $\alpha_{\perp}$ parameters along with their standard deviations that will allow the calculation of the observables D_H/r_s and D_A/r_s.

All of these calculations were done thanks to the clusters to which I was granted access to in Universidad de Córdoba. The hardware used (FQM-378) had the following specifications:

- One node, named Pauli
- One CPU per node, *Intel(R) Xeon(R) Silver 4210R CPU @ 2.40 GHz* with 40 threads
- 64Gb memory
- Operative System: Ubuntu 22.04.2 LTS, release 22.04, codename *jammy*

CHAPTER 4

Results

Using the tools mentioned in the chapter 3, we obtain the data seen in the figure 4.2. Firstly, a template power spectrum $P(k)$ was generated using CLASS. This template stays fixed throughout the calculations, which means its fiducial cosmology will be that of the standard cosmological model. This is, with the six parameters stated in 1.5 and $\Omega_k = 0.00$. Having the template, the BAO are removed using the *remove_bao* routine from montepython, to obtain exactly the plots seen in 3.2.

For this fixed template, 9 different power spectrums were calculated using RUSTICO. We again use the ΛCDM, but this time not assuming a flat universe. Each power spectrum is generated with Ω_k from -0.20 to 0.20, in steps of 0.05, thus yielding the mentioned 9 different power spectrums.

For each one of these Ω_k, the software BRASS was used to calculate each corresponding α, and its standard deviation. This can be seen in the figure 4.2, which presents the $\alpha_{\parallel}$ and $\alpha_{\perp}$ on the first row, the fiducial D_H/r_s, D_A/r_s on the second row and the 'true' D_H/r_s, D_A/r_s for each fiducial cosmology. The superscript $^{fid\,1}$ refers to the fact that Ω_k changes only in the RUSTICO calculations.

These observables, (D_H/r_s and D_A/r_s) were calculated using the definitions (1.13) and (1.15).

The BRASS calculations were done in an iterative way, which means the output from the software was used as the initial condition for the next iteration. To assure better results three iterations were made for each cosmology.

The figure 4.2 shows the results of the calculation of the different observables for different fiducial curvature parameters Ω_k. This chart allows us to observe that the all the calculated observables in the range $\Omega_k \in [-0.20, 0.20]$ are compatible, since they all stand at less than one standard deviation from one another.

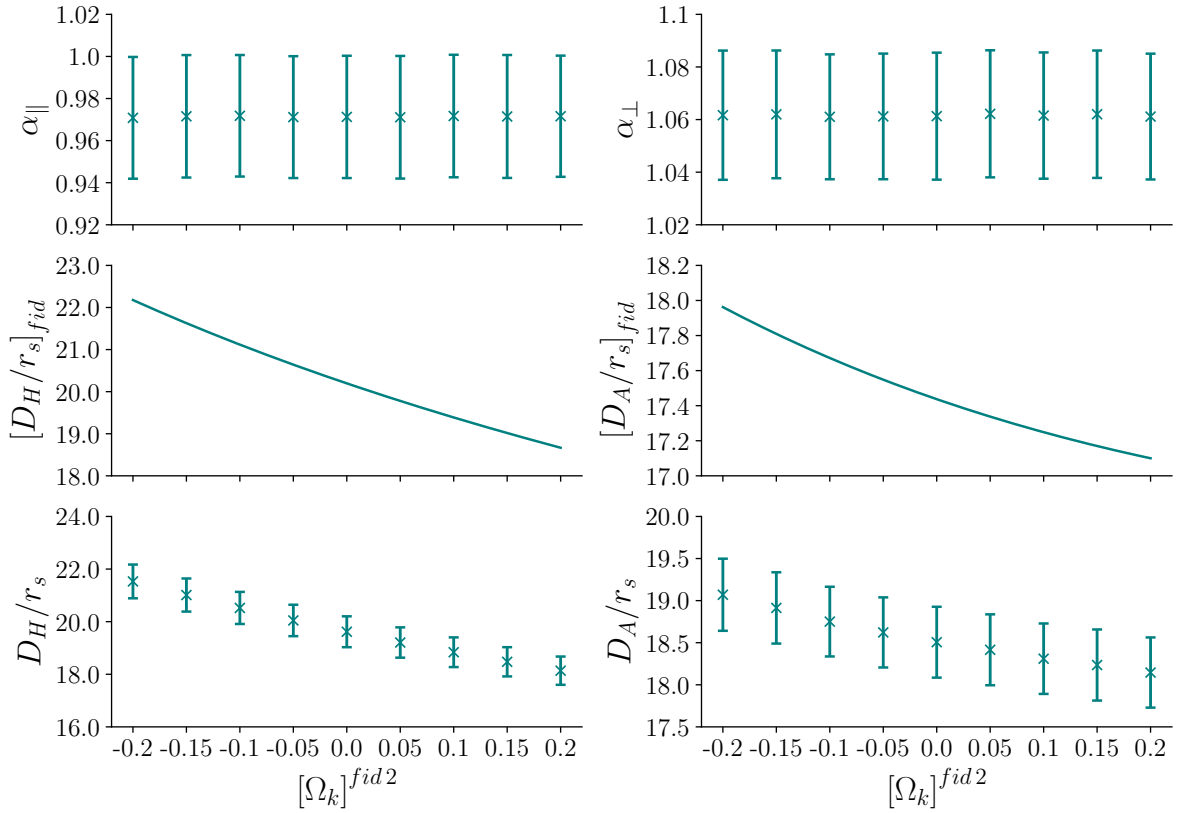

Figura 4.1: Calculations of the different observables D_H/r_s, D_A/r_s, both the fiducial quantities and their actual values for each fiducial curvature parameter Ω_k.

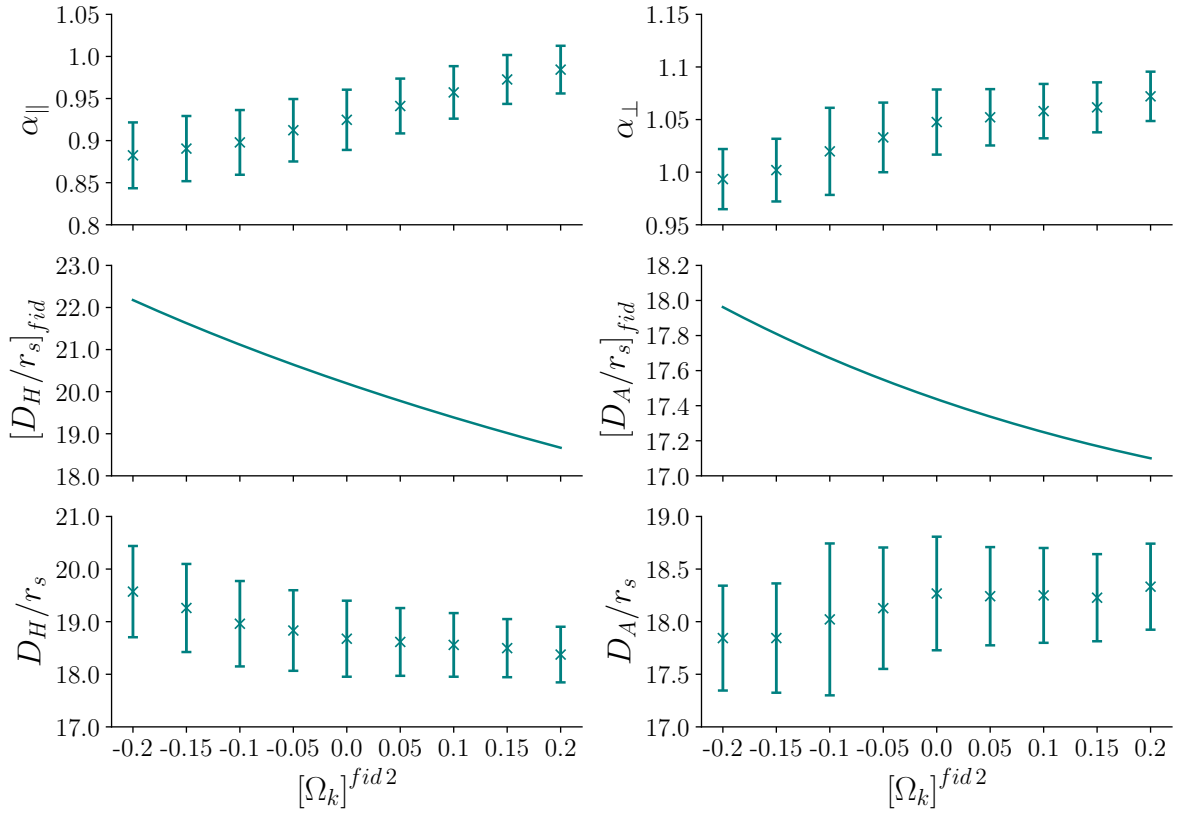

Figura 4.2: Calculations of the different observables D_H/r_s, D_A/r_s, both the fiducial quantities and their actual values for each fiducial curvature parameter Ω_k.

Conclusiones

En este trabajo se ha hecho uso de todas las herramientas mencionadas en el capítulo 3 para calcular la variación de los distintos observables con la curvatura del universo, y verificar así que todos los cálculos que se han hecho hasta ahora (que asumen un universo plano) son válidos. Se ha obtenido en la figura 4.2 que efectivamente para $\Omega_k = 0.00$ ambos parámetros $\alpha_\parallel$ y $\alpha_\perp$ son compatibles con $\alpha = 1$, (debido a que se encuentran a menos de 3σ, siendo σ la varianza de cada α[1].

Además, se puede también observar que la tendencia ascendente de las α contrarresta la tendencia descendiente de D/r_s, lo que indica que variar Ω_k no afecta de manera significativa las mediciones de los observables, de hecho siendo todos estos D/r_s compatibles los unos con los otros, ya que todas las barras de error se superponen.

A pesar de esto, se observa también cierta tendencia descendiente en D_H/r_s para $\Omega_k < 0$, mientras que D_A/r_s se mantiene aproximadamente constante. Esto indica que probablemente sea más acertado escoger $\Omega_k \geq 0$, que $\Omega_k < 0$.

Con esto se puede concluir, que aunque $\Omega_k = 0.00$ es una buena elecciónpara el parámetro de curvatura del universo, se puede variar ligeramente este parámetro de forma que la densidad del universo varíe hasta en un 20% con respecto de la densidad crítica.

[1]No se especifica si $\alpha_\parallel$ o $\alpha_\perp$ ya que se hace referencia a ambas cantidades a la vez. Lo mismo se hará en el siguiente párrafo con D/r_s, que hace referencia tanto a D_H/r_s como a D_A/r_s.

Conclusions

In this work ...

Bibliography

[1] Planck Collaboration. (2018). Planck 2018 results. VI. Cosmological parameters. *Astronomy & Astrophysics*, 641, A6. https://doi.org/10.1051/0004-6361/201833910

[2] Penzias, A. A., & Wilson, R. W. (1965). A Measurement of Excess Antenna Temperature at 4080 Mc/s. *The Astrophysical Journal*, 142, 419. https://doi.org/10.1086/148307

[3] Smoot, G. F., & Mather, J. C. (1992). Structure in the COBE differential microwave radiometer first-year maps. *The Astrophysical Journal*, 396, L1-L5. https://doi.org/10.1086/186504

[4] Cole, S., et al. (The 2dFGRS Collaboration) (2005). The 2dF Galaxy Redshift Survey: power-spectrum analysis of the final dataset and cosmological implications. *Monthly Notices of the Royal Astronomical Society*, 362, 505-534. https://doi.org/10.1111/j.1365-2966.2005.09318.x

[5] Eisenstein, D. J., et al. (The SDSS Collaboration) (2005). Detection of the Baryon Acoustic Peak in the Large-Scale Correlation Function of SDSS Luminous Red Galaxies. *The Astrophysical Journal, 633, 560-574*. https://doi.org/10.1086/466512

[6] Hubble, E. (1929). A relation between distance and radial velocity among extragalactic nebulae. *Proceedings of the National Academy of Sciences*, 15(3), 168-173. https://doi.org/10.1073/pnas.15.3.168

[7] Lesgourgues, J., Tram, T., & Sprenger, T. The Cosmic Linear Anisotropy Solving System (CLASS) IV: efficient implementation of the Cosmic Microwave Background and large scale structure likelihoods. *Journal of Cosmology and Astroparticle Physics*, 2011(07), 002. https://github.com/lesgourg/class_public.

[8] Brinckmann, T. Montepython: Pythonic MCMC for Cosmology. *Journal of Open Source Software*, 3(24), 676, 2018. https://github.com/montepython/montepython_public.

[9] Gil-Marín, H. RUSTICO: A fast and scalable method for measuring the autocorrelation function of galaxy surveys. *Astronomy and Computing*, 31, 100391, 2020. https://github.com/Hector-Gil-Marina/rustico.

[10] Gil-Marín, H. BRASS: BAO and RSD Analysis of Spectra with Systematics. *Journal of Open Source Software*, 4(45), 1884, 2019. https://github.com/brass-project/brass.

[11] S. Alam *et al.* [eBOSS], Phys. Rev. D **103**, no.8, 083533 (2021) doi:10.1103/PhysRevD.103.083533 [arXiv:2007.08991 [astro-ph.CO]].

Anexo: Ejemplo para introducir código Matlab

```
%% 3-D Plots
% Three-dimensional plots typically display a surface
% defined by a function in two variables, z = f(x,y) .
%%
% To evaluate z, first create a set of (x,y) points
% over the domain of the function using meshgrid.
    [X,Y] = meshgrid(-2:.2:2);
    Z = X .* exp(-X.^2 - Y.^2);
%%
% Then, create a surface plot.
    surf(X,Y,Z)
%%
% Both the surf function and its companion mesh display
% surfaces in three dimensions. surf displays both the
% connecting lines and the faces of the surface in color.
% Mesh produces wireframe surfaces that color only the
%lines connecting the defining points.
```

Anexo: Ejemplo para introducir código ISE

```
1  library IEEE;
2              use IEEE.STD_LOGIC_1164.ALL;
3              use IEEE.STD_LOGIC_ARITH.ALL;
4              use IEEE.STD_LOGIC_UNSIGNED.ALL;
5  -- Uncomment the following library declaration if
6  -- instantiating  any Xilinx primitive in this code.
7  -- library UNISIM;
8  -- use UNISIM.VComponents.all;
9
10 entity counter is
11     Port ( CLOCK : in  STD_LOGIC;
12     DIRECTION :    in  STD_LOGIC;
13     COUNT_OUT :    out STD_LOGIC_VECTOR (3 downto 0));
14 end counter;
15
16 architecture Behavioral of counter is
17 signal count_int : std_logic_vector(3 downto 0) := "0000";
18 begin
19 process (CLOCK)
20 begin
21     if CLOCK='1' and CLOCK'event then
22         if DIRECTION='1' then
23             count_int <= count_int + 1;
24         else
25             count_int <= count_int - 1;
26         end if;
27     end if;
28 end process;
29 COUNT_OUT <= count_int;
30 end Behavioral;
```